

Angular Momentum Generation from Holographic Chern-Simons Models

Chaolun Wu

*Kadanoff Center for Theoretical Physics and Enrico Fermi Institute
University of Chicago, Chicago, Illinois 60637, USA*

Email: chaolunwu@uchicago.edu

Abstract

We study parity-violating effects, particularly the generation of angular momentum density and its relation to the parity-odd and dissipationless transport coefficient Hall viscosity, in strongly-coupled quantum fluid systems in 2+1 dimensions using holographic method. We employ a class of 3+1-dimensional holographic models of Einstein-Maxwell system with gauge and gravitational Chern-Simons terms coupled to a dynamical scalar field. The scalar can condensate and break the parity spontaneously. We find that when the scalar condensates, a non-vanishing angular momentum density and an associated edge current are generated, and they receive contributions from both gauge and gravitational Chern-Simons terms. The angular momentum density does not satisfy a membrane paradigm form because the vector mode fluctuations from which it is calculated are effectively massive. On the other hand, the emergence of Hall viscosity is a consequence of the gravitational Chern-Simons term alone and it has membrane paradigm form. We present both general analytic results and numeric results which take back-reactions into account. The ratio between Hall viscosity and angular momentum density resulting from the gravitational Chern-Simons term has in general a deviation from the universal $1/2$ value obtained from field theory and condensed matter physics.

Contents

1	Introduction	2
2	Holographic Chern-Simons Models	4
2.1	Bulk and Boundary Actions	4
2.2	Perturbative Expansion of Bulk Action	6
2.3	Equations of Motion and Background	7
3	Vector Mode Fluctuations and Angular Momentum Density	8
3.1	Formula for Angular Momentum Density	8
3.2	First Order On-Shell Action	9
3.3	Vector Mode Fluctuations and Angular Momentum Density	11
3.4	Effective Masses and Membrane Paradigm Violation	13
4	Tensor Mode Fluctuations and Hall Viscosity	15
4.1	Tensor Mode EOMs and Solutions	15
4.2	2-Point Functions and Viscosities	16
5	Numeric Results of the Axion Condensate Phase	17
5.1	Gravitational Chern-Simons Model: The Probe Limit	18
5.2	Gravitational Chern-Simons Model: Including Back-reactions	19
5.3	Gauge Chern-Simons Model: Angular Momentum Density	22
6	Conclusions and Comments	23
	Acknowledgments	24
	References	24

1 Introduction

When parity is broken, additional transport phenomena can take place and reveal interesting underlying dynamical and topological structures of the systems. Quantum Hall effect is a well known example. In fact, in 2+1 dimensions, when parity is broken, in addition to Hall conductivity, a few other parity-odd transport coefficients can also arise. These transport coefficients had been systematically studied in [1] for relativistic fluids and recently in [2] for non-relativistic fluids. Among them, Hall viscosity is the dissipationless and parity-odd cousin of shear viscosity, just like Hall conductivity can be viewed similarly compared to ordinary (longitudinal) conductivity. The effect of Hall viscosity can be interpreted as a Lorentz-type force (sometimes called the “Lorentz shear force”) acting perpendicular to the shear flow. Hall viscosity was first studied for various quantum Hall states [3–9] and then for chiral superfluid states [7, 9] and topological insulators [10, 11]. It was also studied

using general approaches such as linear response theory [12], effective field theories [13–16], viscoelastic-electromagnetism [17] and quantum hydrodynamics of vortex flow [18–20]. It was first noticed in [7, 9] and later re-derived using more general methods in [12, 14, 16] that Hall viscosity is equal to a half of the orbital spin density of the systems. In the absence of mechanical rotation or spin-orbit coupling, this is the total angular momentum density of the system. This reveals another interesting effect when parity is broken – the generation of angular momentum density and edge current. The microscopic origin of such an angular momentum density varies for different systems, but the common feature is the formation of vortices. For quantum Hall states, this is from the cyclotron motion of the electrons or quasi-particles in magnetic field. For chiral superfluids, this is due to the relative orbital angular momentum of the two paired electrons in Cooper pairs [21–23]. The effect of the non-vanishing angular momentum density and Hall viscosity is to accumulate momentum and charges on the boundaries [18] and to induce an edge current.

Over the last decade, the gauge/gravity correspondence [24–26] has often offered new insights to the understanding of strongly-coupled quantum systems, such as quark-gluon plasma, superconductors, superfluids, quantum Hall effects and topological insulators, just to name a few. In this paper we are trying to understand the generation of angular momentum density and its relation to Hall viscosity in 2+1-dimensional strongly-coupled systems from the holographic point of view. In [27] a holographic model with dynamical gravitational Chern-Simons term was first used to calculate Hall viscosity. This model was further upgraded and numerically computed in [28, 29]. Recently [30, 31] studied both Hall viscosity and Curl viscosity using similar holographic models with Chern-Simons terms. Spontaneous generation of angular momentum from holographic models with gauge and gravitational Chern-Simons terms was also studied in [32, 33], and more recently in [34], with focus on gapless systems. The common feature of all these studies is that in their holographic actions, there are Chern-Simons terms (gauge [35, 36] or gravitational [37], or both) coupled to a dynamical axion scalar field, which break parity when the axion condensates. However, none of them reported to find both Hall viscosity and angular momentum density at the same time, thus does not yield a unified picture of them as that from the studies using non-holographic approaches [7, 9, 13, 14, 16]. Recently, [38] studied a different class of model – the holographic $p_x + ip_y$ model of [39]. They found both non-vanishing Hall viscosity and angular momentum density in the superfluid phase, and showed that the ratio between Hall viscosity and angular momentum density is a constant, at least near the critical regime, and is numerically consistent with being 1/2 in the probe limit regime. This suggests an agreement with previous results from [7, 9, 13, 14, 16]. In fact, the holographic $p_x + ip_y$ model can be viewed as a dual description to chiral superfluid states, like those studied in [21–23], and it was from computing Hall viscosity for such states (among others) that [7] first pointed out the relation between Hall viscosity and angular momentum density. The holographic $p_x + ip_y$ model is different from those Chern-Simons models in [27–30, 32] that it does not contain Chern-Simons terms in the action, so the action is perfectly parity-preserving. But the ground state breaks spatial parity by locking it to non-Abelian gauge parity, which is broken by the appearance of non-Abelian gauge connection, and this is the only source for the emergence of Hall viscosity, angular momentum density, and Hall conductivity (studied numerically earlier in [40]). Thus in holographic $p_x + ip_y$ model all the parity-odd transport coefficients and angular momentum are generated in a unified way.

In this paper, we go back to the holographic gauge and gravitational Chern-Simons models, and compute the angular momentum density using the method proposed in [38]. It is worth noting that [33] offers an alternative execution of the computation for angular momentum density, and our general analytical results agree. We will show that there is indeed a generation of angular momentum density accompanying the emergence of Hall viscosity when the axion scalar condensates spontaneously breaks parity. The angular momentum density receives contributions from both the gauge and gravitational Chern-Simons terms. It does not have a membrane paradigm form and part of its expression is a bulk integral from the black hole horizon to the boundary. The origin of this is that the vector mode fluctuations from which the angular momentum density is calculated acquire effective masses through mutual coupling in a non-trivial charged black hole background. On contrary, the Hall viscosity has a membrane paradigm form because the tensor mode fluctuations from which it is calculated remain massless. The ratio between Hall viscosity and angular momentum density resulting from the gravitational Chern-Simons term is not exactly a fixed constant, but remains more or less unchanged as temperature is varied, except at the very low temperature regime. The ratio depends on conformal dimension of the condensate that breaks parity spontaneously.

The paper is organized as following. In section 2, we give the general formalism of the holographic Chern-Simons models we are using and the ground state ansatz. In section 3 and 4, we compute vector mode and tensor mode fluctuations to obtain angular momentum density and Hall viscosity, respectively. In section 5, we present numeric results for the axion condensate phase, first in the probe limit and then to include back-reactions. Conclusions and comments follow in section 6. Through out this paper, we will work in 3+1 spacetime dimensions.

2 Holographic Chern-Simons Models

For a general review on Chern-Simons modified gravity theory, we refer readers to [41]. In this section, we will only list key ingredients relevant to the calculation of Hall viscosity and angular momentum.

2.1 Bulk and Boundary Actions

The bulk action of our holographic Chern-Simons model in 3+1 dimension is:

$$S_{\text{bulk}} = \frac{1}{2\kappa^2} \int d^4x \sqrt{-g} \left\{ R - 2\Lambda - \frac{1}{4} F_{\mu\nu}^2 \right\} + S_{\vartheta} + S_{\text{CS}} + S_{\text{CS}}^A, \quad (2.1)$$

where $F_{\mu\nu} = \partial_\mu A_\nu - \partial_\nu A_\mu$ is the field strength of Maxwell field. The cosmological constant $\Lambda = -3/L^2$ and L is the AdS radius. The real (pseudo) scalar ϑ 's action is

$$S_{\vartheta} = \frac{1}{2\kappa^2} \int d^4x \sqrt{-g} \left\{ -\frac{1}{2} (\partial\vartheta)^2 - V[\vartheta] \right\}. \quad (2.2)$$

We choose the potential to be

$$V[\vartheta] = \frac{1}{2} m^2 \vartheta^2 + \frac{1}{4} c_4 \vartheta^4, \quad (2.3)$$

though in the actual calculation we will try to keep $V[\vartheta]$ general and not to implement this form until we have to.

Abelian gauge Chern-Simons term is

$$S_{\text{CS}}^A = \frac{1}{2\kappa^2} \int d^4x \sqrt{-g} \left\{ \frac{\lambda_A}{4} \Theta_A[\vartheta] {}^*FF \right\}, \quad (2.4)$$

where λ_A is the coupling constant,

$${}^*FF = {}^*F^{\mu\nu} F_{\mu\nu}, \quad (2.5)$$

and the dual field strength is

$${}^*F^{\mu\nu} = \frac{1}{2} \epsilon^{\mu\nu\alpha\beta} F_{\alpha\beta}. \quad (2.6)$$

$\Theta_A[\vartheta]$ is a general functional of ϑ .

The gravitational Chern-Simons term is

$$S_{\text{CS}} = \frac{1}{2\kappa^2} \int d^4x \sqrt{-g} \left\{ -\frac{\lambda}{4} \Theta[\vartheta] {}^*RR \right\}, \quad (2.7)$$

where λ is the coupling constant and the Pontryagin density is defined as

$${}^*RR = {}^*R^{\mu\nu\rho\sigma} R_{\nu\mu\rho\sigma}, \quad (2.8)$$

and the dual Riemann tensor is

$${}^*R^{\mu\nu\rho\sigma} = \frac{1}{2} \epsilon^{\rho\sigma\eta\zeta} R^{\mu\nu}{}_{\eta\zeta}, \quad (2.9)$$

where $\epsilon^{\rho\sigma\eta\zeta}$ is the Levi-Civita tensor. We choose the convention¹ $\epsilon_{txyz} = \sqrt{-g}$. $\Theta[\vartheta]$ is a general functional of ϑ . Again we will try to keep its form general for as long as possible in our calculation. A more detailed discussion of its form will be presented in Section 5.

The boundary terms include the Gibbons-Hawking term

$$S_{\text{GH}} = \frac{1}{\kappa^2} \int_{\text{boundary}} d^3x \sqrt{-\gamma} K \quad (2.10)$$

and a counter term

$$S_{\text{ct}} = -\frac{2}{\kappa^2 R} \int_{\text{boundary}} d^3x \sqrt{-\gamma}, \quad (2.11)$$

where \hat{n}_μ is the outgoing unit normal 1-form of the boundary and $\gamma_{\mu\nu} = g_{\mu\nu} - \hat{n}_\mu \hat{n}_\nu$ is the induced metric on the boundary. The extrinsic curvatures are $K_{\mu\nu} = \gamma_\mu^\rho \gamma_\nu^\sigma \nabla_\rho \hat{n}_\sigma$ and $K = K_\mu^\mu$. There is also a Chern-Simons boundary term, analog to Gibbons-Hawking term, added such that the Dirichlet boundary value problem is well posed:

$$S_{\partial\text{CS}} = \frac{1}{2\kappa^2} \int_{\text{boundary}} d^3x \sqrt{-\gamma} \left\{ -\lambda \Theta[\vartheta] \hat{n}_\rho \epsilon^{\rho\sigma\gamma\delta} K_\sigma{}^\eta \nabla_\gamma K_{\delta\eta} \right\}. \quad (2.12)$$

¹Our convention for $\epsilon^{\rho\sigma\eta\zeta}$ differs from that of [27, 38] by a sign, thus the corresponding terms in both the Kubo formula and 2-point functions differ by a sign, but the final expression for Hall viscosity remains the same because these two signs cancel.

2.2 Perturbative Expansion of Bulk Action

To compute 2-point functions, we perturbatively expand the on-shell actions around the background up to second order in field fluctuations. The background and fluctuations are

$$\begin{aligned} g_{\mu\nu} &= \bar{g}_{\mu\nu} + h_{\mu\nu}, \\ A_\mu &= \bar{A}_\mu + a_\mu, \\ \vartheta &= \bar{\theta} + \delta\theta, \end{aligned} \tag{2.13}$$

where $\bar{g}_{\mu\nu}$, \bar{A}_μ and $\bar{\theta}$ are the background and $h_{\mu\nu}$, a_μ and $\delta\theta$ are fluctuations.² To fully consider the back-reactions of the gauge fields on the metric, we assume $h_{\mu\nu}$, a_μ and $\delta\theta$ are of the same order. We also define the short-hand notations:

$$\Theta[\vartheta] = \bar{\Theta} + \delta\Theta, \quad \text{where} \quad \bar{\Theta} = \Theta[\bar{\theta}], \quad \delta\Theta = \left. \frac{\delta\Theta[\vartheta]}{\delta\vartheta} \right|_{\vartheta=\bar{\theta}} \delta\theta, \tag{2.14}$$

and similarly for $\Theta_A[\vartheta]$. The first order on-shell action which is linear in fluctuations is

$$\begin{aligned} S_{\text{bulk}}^{(1)} &= \frac{1}{2\kappa^2} \int d^4x \partial_\mu \left\{ \sqrt{-\bar{g}} \left(\bar{\nabla}_\nu h^{\mu\nu} - \bar{\nabla}^\mu h - \bar{F}^{\mu\nu} a_\nu + \lambda_A \bar{\Theta}_A {}^* \bar{F}^{\mu\nu} a_\nu \right. \right. \\ &\quad \left. \left. - \delta\theta \bar{\nabla}^\mu \bar{\theta} - \lambda \bar{\Theta} {}^* \bar{R}^{\nu\alpha\mu\beta} \bar{\nabla}_\nu h_{\alpha\beta} + \lambda h_{\alpha\beta} {}^* \bar{R}^{\mu\alpha\nu\beta} \bar{\nabla}_\nu \bar{\Theta} \right) \right\}. \end{aligned} \tag{2.15}$$

The second order on-shell action quadratic in fluctuations is

$$\begin{aligned} S_{\text{bulk}}^{(2)} &= \frac{1}{4\kappa^2} \int d^4x \partial_\mu \left\{ \sqrt{-\bar{g}} \left[\frac{1}{2} h \bar{\nabla}_\nu h^{\mu\nu} + \frac{3}{2} h^{\mu\nu} \bar{\nabla}_\nu h - h^{\rho\sigma} \bar{\nabla}_\rho h_\sigma^\mu - 2h^{\mu\rho} \bar{\nabla}^\sigma h_{\rho\sigma} \right. \right. \\ &\quad \left. \left. + \frac{3}{2} h^{\rho\sigma} \bar{\nabla}^\mu h_{\rho\sigma} - \frac{1}{2} h \bar{\nabla}^\mu h - a_\nu \left(\frac{1}{2} \bar{F}^{\mu\nu} h + \bar{F}_\rho^{[\mu} h^{\nu]\rho} + F^{(1)\mu\nu} \right) \right. \right. \\ &\quad \left. \left. + \left(h^{\mu\nu} - \frac{1}{2} \bar{g}^{\mu\nu} h \right) \delta\theta \bar{\nabla}_\nu \bar{\theta} - \delta\theta \bar{\nabla}^\mu \delta\theta \right] \right\} \\ &\quad + \frac{\lambda}{4\kappa^2} \int d^4x \partial_\mu \left\{ \sqrt{-\bar{g}} \left[\frac{1}{2} \bar{\Theta} {}^* \bar{R}^{\nu\alpha\mu\beta} h_\alpha^\sigma \left(\bar{\nabla}_\beta h_{\sigma\nu} + \bar{\nabla}_{[\nu} h_{\sigma]\beta} \right) + \bar{\Theta} {}^* \bar{R}^{\nu\rho\mu\beta} h_\rho^\alpha \bar{\nabla}_\nu h_{\alpha\beta} \right. \right. \\ &\quad \left. \left. - h_{\alpha\beta} h_\rho^\alpha {}^* \bar{R}^{\mu\rho\nu\beta} \bar{\nabla}_\nu \bar{\Theta} - \frac{1}{2} \bar{\Theta} \bar{\epsilon}^{\mu\beta\gamma\delta} \left(\bar{\nabla}_\gamma \bar{\nabla}_\delta h^{\nu\alpha} + \bar{\nabla}_\gamma \bar{\nabla}^{[\alpha} h_\delta^{\nu]} \right) \bar{\nabla}_\nu h_{\alpha\beta} \right. \right. \\ &\quad \left. \left. + \frac{1}{2} \bar{\epsilon}^{\nu\beta\gamma\delta} \left(\bar{\nabla}_\nu \bar{\Theta} \right) h_{\alpha\beta} \left(\bar{\nabla}_\gamma \bar{\nabla}_\delta h^{\mu\alpha} + \bar{\nabla}_\gamma \bar{\nabla}^{[\alpha} h_\delta^{\mu]} \right) - {}^* \bar{R}^{\nu\alpha\mu\beta} \delta\theta \bar{\nabla}_\nu h_{\alpha\beta} \right. \right. \\ &\quad \left. \left. + {}^* \bar{R}^{\mu\alpha\nu\beta} h_{\alpha\beta} \bar{\nabla}_\nu \delta\theta \right] \right\} \\ &\quad + \frac{\lambda_A}{2\kappa^2} \int d^4x \partial_\mu \left\{ \sqrt{-\bar{g}} \left[\delta\Theta_A {}^* \bar{F}^{\mu\nu} a_\nu + \bar{\Theta}_A {}^* F^{(1)\mu\nu} a_\nu \right] \right\}. \end{aligned} \tag{2.16}$$

²For axion, ϑ is the whole field, which equals background plus fluctuation. $\bar{\theta}$ is the background part, which is the same as $\theta(z)$ as defined in (2.22) to emphasize the z-dependence. $\delta\theta$ is the fluctuation. θ_0 and θ_1 are the coefficients of non-normalizable and normalizable modes of bulk background solution of the axion, as defined in (3.10).

Here all co-variant derivatives $\bar{\nabla}$ and raising and lowering indices are with respect to the background metric $\bar{g}_{\mu\nu}$, with $h \equiv h_\mu^\mu$ and $F_{\mu\nu}^{(1)} \equiv \bar{\nabla}_{[\mu} a_{\nu]}$.³ These actions are written as integrals of total derivatives, which means they are boundary terms.

2.3 Equations of Motion and Background

The EOMs are

$$R_{\mu\nu} - \frac{1}{2}Rg_{\mu\nu} + \Lambda g_{\mu\nu} + \lambda C_{\mu\nu} = \frac{1}{2}T_{\mu\nu}, \quad (2.17)$$

$$\nabla_\mu (F^{\mu\nu} - \lambda_A \bar{\Theta}_A {}^* \bar{F}^{\mu\nu}) = 0, \quad (2.18)$$

$$\nabla^2 \vartheta - \frac{\delta V}{\delta \vartheta} - \frac{\lambda}{4} \frac{\delta \Theta}{\delta \vartheta} {}^* R R + \frac{\lambda_A}{4} \frac{\delta \Theta_A}{\delta \vartheta} {}^* F F = 0, \quad (2.19)$$

where

$$\begin{aligned} C_{\mu\nu} &= \frac{1}{2} \nabla^\alpha \nabla^\beta (\Theta {}^* R_{\alpha\mu\beta\nu} + \Theta {}^* R_{\alpha\nu\beta\mu}) \\ &= \frac{1}{2} \left[(\nabla^\alpha \nabla^\beta \Theta) {}^* R_{\alpha\mu\beta\nu} + (\nabla^\beta \Theta) \epsilon_{\beta\mu\gamma\delta} (\nabla^\gamma R_\nu^\delta) \right] + (\mu \leftrightarrow \nu) \end{aligned} \quad (2.20)$$

and

$$T_{\mu\nu} = \left[F_{\mu\rho} F_\nu{}^\rho - \frac{1}{4} g_{\mu\nu} F^2 \right] + \left[(\nabla_\mu \vartheta) (\nabla_\nu \vartheta) - \frac{1}{2} g_{\mu\nu} (\nabla \vartheta)^2 - g_{\mu\nu} V[\vartheta] \right]. \quad (2.21)$$

We choose the background ansatz to be

$$\begin{cases} d\bar{s}^2 = -F(z) dt^2 + \frac{dz^2}{F(z)} + r(z)^2 (dx^2 + dy^2) \\ \bar{A} = \Phi(z) dt, \quad \bar{\theta} = \theta(z) \end{cases}. \quad (2.22)$$

The temperature is given by $F(z) = 4\pi T(z - z_H) + O((z - z_H)^2)$ and $\Phi(z) = O(z - z_H)$ near the horizon $z = z_H$. The boundary is at $z = \infty$.

The background EOMs are

$$\frac{d^2 r(z)}{dz^2} + \frac{1}{4} r(z) \left(\frac{d\theta(z)}{dz} \right)^2 = 0, \quad (2.23)$$

$$\frac{d^2 F(z)}{dz^2} - \frac{2F(z)}{r(z)^2} \left(\frac{dr(z)}{dz} \right)^2 - \left(\frac{d\Phi(z)}{dz} \right)^2 + \frac{F(z)}{2} \left(\frac{d\theta(z)}{dz} \right)^2 = 0, \quad (2.24)$$

$$\frac{d^2 \Phi(z)}{dz^2} + \frac{2}{r(z)} \frac{dr(z)}{dz} \frac{d\Phi(z)}{dz} = 0, \quad (2.25)$$

$$\frac{d}{dz} \left[r(z)^2 F(z) \left(\frac{d}{dz} \theta(z) \right) \right] - r(z)^2 \frac{\delta V[\theta]}{\delta \theta} = 0. \quad (2.26)$$

³In this paper we define the symmetrization $A_{(\mu} B_{\nu)} \equiv A_\mu B_\nu + A_\nu B_\mu$ and the anti-symmetrization $A_{[\mu} B_{\nu]} \equiv A_\mu B_\nu - A_\nu B_\mu$ without the factor of $\frac{1}{2}$.

and a constraint equation from the trace of Einstein equation:

$$\begin{aligned} \frac{d^2 F(z)}{dz^2} + 4 \frac{F(z)}{r(z)} \frac{d^2 r(z)}{dz^2} + 2 \frac{F(z)}{r(z)^2} \left(\frac{dr(z)}{dz} \right)^2 + \frac{4}{r(z)} \frac{dF(z)}{dz} \frac{dr(z)}{dz} \\ + \frac{1}{2} F(z) \left(\frac{d\theta(z)}{dz} \right)^2 + 2V[\theta] = \frac{12}{L^2}. \end{aligned} \quad (2.27)$$

3 Vector Mode Fluctuations and Angular Momentum Density

3.1 Formula for Angular Momentum Density

In this section, we follow the method proposed in [38] to calculate the angular momentum density. The gauge conditions are chosen to be $h_{\mu z} = a_z = 0$. We need to study only the static case, so all fluctuations are time-independent. For completeness, we first review the derivation of the formula used to compute angular momentum density. The metric at the boundary is $\gamma_{\alpha\beta} = \eta_{\alpha\beta} + \delta\gamma_{\alpha\beta}$, where $\eta_{\alpha\beta} = (-1, 1, 1)$ is the flat Lorentzian metric and $\delta\gamma_{\alpha\beta} = \bar{h}_{\alpha\beta}$ is the metric fluctuation at the boundary. $\alpha, \beta = t, x, y$ and $i, j, k = x, y$. The energy-stress tensor is defined as

$$T^{\alpha\beta} = \frac{2}{\sqrt{-\gamma}} \frac{\delta S}{\delta \gamma_{\alpha\beta}} \Big|_{\gamma_{\alpha\beta} = \eta_{\alpha\beta}}. \quad (3.1)$$

Then the linearized (first order) on-shell action we calculate from holography will in general takes the form

$$S^{(1)} = \frac{1}{2} \int d^3 x \bar{h}_{\alpha\beta}(x) T^{\alpha\beta}(x). \quad (3.2)$$

The $\beta = t$ component of the conservation law $\nabla_\alpha T^{\alpha\beta} = 0$ in the static case and flat background reads

$$\partial_i T^{ti}(\vec{x}) = 0, \quad (3.3)$$

which has a general solution

$$T^{ti}(\vec{x}) = \frac{1}{2} \epsilon^{ij} \partial_j \ell(\vec{x}), \quad (3.4)$$

where $\epsilon^{xy} = -\epsilon^{yx} = 1$, $\epsilon^{xx} = \epsilon^{yy} = 0$ and $\ell(\vec{x})$ is an arbitrary function. It is straightforward to see that $\ell(\vec{x})$ is the angular momentum density by definition:

$$L = \int d^2 \vec{x} \epsilon_{ij} x^i T^{tj}(\vec{x}) = \frac{1}{2} \int d^2 \vec{x} \epsilon_{ij} x^i \epsilon^{jk} \partial_k \ell(\vec{x}) = \int_V d^2 \vec{x} \ell(\vec{x}), \quad (3.5)$$

where in the last step we have integrated by parts, assumed that the system and hence $\ell(\vec{x})$ are localized in a finite volume V , and used $\epsilon_{ij} \epsilon^{jk} = -\delta_i^k$. At the end the volume V can be extended to include the whole space. Plug (3.4) into (3.2), turn on only $\bar{h}_{ti}(\vec{x})$ fluctuation and integrate by parts, we get

$$S^{(1)} = \frac{1}{2} \int d^3 x \ell(\vec{x}) \epsilon^{ij} \partial_i \bar{h}_{tj}(\vec{x}). \quad (3.6)$$

When the system is homogeneous, $\ell(\vec{x}) = \ell$ is a constant and can be factored out of the integral. Then we have

$$S^{(1)} = \frac{\ell}{2} \int d^3x \left(\frac{\partial}{\partial x} \bar{h}_{ty}(\vec{x}) - \frac{\partial}{\partial y} \bar{h}_{tx}(\vec{x}) \right). \quad (3.7)$$

(3.6) and (3.7) are the template formulae for computing angular momentum density in holography.

3.2 First Order On-Shell Action

We now calculate the linearized on-shell action $S^{(1)} = S_{\text{bulk}}^{(1)} + S_{\text{GH}}^{(1)} + S_{\partial\text{CS}}^{(1)} + S_{\text{ct}}^{(1)}$. The first part of the contribution is from the z -derivative term in $S_{\text{bulk}}^{(1)}$ plus the boundary terms:

$$\begin{aligned} & \frac{1}{2\kappa^2} \int_{z=\infty} d^3x \left\{ 2r(z) \left(F(z) \frac{dr(z)}{dz} - \frac{r(z)}{L} \sqrt{F(z)} \right) h_t^t(\vec{x}, z) + r(z)^2 \frac{d\Phi(z)}{dz} a_t(\vec{x}, z) \right. \\ & + r(z) \left(F(z) \frac{dr(z)}{dz} + \frac{r(z)}{2} \frac{dF(z)}{dz} - \frac{2r(z)}{L} \sqrt{F(z)} \right) \left(h_x^x(\vec{x}, z) + h_y^y(\vec{x}, z) \right) \\ & - r(z)^2 F(z) \frac{d\theta(z)}{dz} \delta\theta(\vec{x}, z) \\ & + \frac{\lambda}{2} \bar{\Theta}(z) \frac{dr(z)}{dz} \left(2F(z) \frac{dr(z)}{dz} - r(z) \frac{dF(z)}{dz} \right) \left(\frac{\partial}{\partial x} h_t^y(\vec{x}, z) - \frac{\partial}{\partial y} h_t^x(\vec{x}, z) \right) \\ & \left. + \frac{\lambda}{4} \bar{\Theta}(z) r(z) \left(2F(z) \frac{dr(z)}{dz} - r(z) \frac{dF(z)}{dz} \right) \left(\frac{\partial^2}{\partial z \partial x} h_t^y(\vec{x}, z) - \frac{\partial^2}{\partial z \partial y} h_t^x(\vec{x}, z) \right) \right\}. \end{aligned} \quad (3.8)$$

Using the asymptotic behavior of the metric:

$$\begin{cases} r(z) = \frac{z}{L} + O\left(\frac{1}{z^3}\right) \\ F(z) = \left(\frac{z}{L}\right)^2 + \frac{\Gamma}{z} + O\left(\frac{1}{z^2}\right), \\ \Phi(z) = \Phi_0 + \frac{\Phi_1}{z} + O\left(\frac{1}{z^2}\right) \end{cases} \quad (3.9)$$

the first two lines of the integrand in (3.8) are

$$\frac{\Gamma}{2L^2} \left(2\bar{h}_t^t - \bar{h}_x^x - \bar{h}_y^y \right) - \frac{\Phi_1}{L^2} \bar{a}_t.$$

Since we do not turn on these boundary fields, they have no contribution. The axion has near-boundary behavior

$$\theta(z) = \theta_0 z^{-\Delta_-} \dots + \theta_1 z^{-\Delta_+} \dots, \quad (3.10)$$

where

$$\Delta_{\pm} = \frac{3}{2} \pm \sqrt{\frac{9}{4} + m^2 L^2}. \quad (3.11)$$

The first coefficient θ_0 is equal to the source J and the second coefficient θ_1 equal to the condensate $\langle \mathcal{O} \rangle$. Since we are considering a sourceless case, we set $\theta_0 = 0$. The axion fluctuation $\delta\theta$ has similar near-boundary behavior:

$$\delta\theta = \delta\bar{\theta}z^{-\Delta_-} + \dots,$$

then the third line in (3.8) becomes

$$\frac{\Delta_+}{L^4}\theta_1\delta\bar{\theta},$$

which has no contribution because $\delta\bar{\theta}$ is turned off. Thus the first part's contribution is only from the last two lines in (3.8):

$$\begin{aligned} & \frac{\lambda}{4\kappa^2} \int_{z=\infty} d^3x \left\{ \bar{\Theta}(z) \frac{dr(z)}{dz} \left(2F(z) \frac{dr(z)}{dz} - r(z) \frac{dF(z)}{dz} \right) \left(\frac{\partial}{\partial x} h_t^y(\vec{x}, z) - \frac{\partial}{\partial y} h_t^x(\vec{x}, z) \right) \right. \\ & \left. + \frac{1}{2} \bar{\Theta}(z) r(z) \left(2F(z) \frac{dr(z)}{dz} - r(z) \frac{dF(z)}{dz} \right) \left(\frac{\partial^2}{\partial z \partial x} h_t^y(\vec{x}, z) - \frac{\partial^2}{\partial z \partial y} h_t^x(\vec{x}, z) \right) \right\}. \quad (3.12) \end{aligned}$$

The second part of the contribution to $S^{(1)}$ is from the x - and y -derivative terms in $S_{\text{bulk}}^{(1)}$. The part involving scalar and tensor mode fluctuations are quadratic in spatial derivatives:

$$\frac{1}{2\kappa^2} \int d^4x \left\{ - \left(\frac{\partial^2}{\partial x^2} + \frac{\partial^2}{\partial y^2} \right) h_t^t(\vec{x}, z) - \frac{\partial^2}{\partial y^2} h_x^x(\vec{x}, z) - \frac{\partial^2}{\partial x^2} h_y^y(\vec{x}, z) + 2 \frac{\partial^2}{\partial x \partial y} h_y^x(\vec{x}, z) \right\},$$

thus is of higher order. The part involving vector mode fluctuations will give the main contribution:

$$\begin{aligned} & \frac{\lambda}{4\kappa^2} \int d^4x \left\{ \left[\left(r(z)^2 \frac{d}{dz} \left(\frac{1}{r(z)} \frac{dr(z)}{dz} \frac{dF(z)}{dz} \right) - 4F(z) \frac{dr(z)}{dz} \frac{d^2r(z)}{dz^2} \right) \bar{\Theta}(z) \right. \right. \\ & \left. \left. + r(z)^3 \left(\frac{d}{dz} \frac{F(z)}{r(z)^2} \right) \frac{dr(z)}{dz} \frac{d\bar{\Theta}(z)}{dz} \right] \left(\frac{\partial}{\partial x} h_t^y(\vec{x}, z) - \frac{\partial}{\partial y} h_t^x(\vec{x}, z) \right) \right. \\ & \left. + r(z) \bar{\Theta}(z) \left[r(z)^2 \frac{d}{dz} \left(\frac{1}{r(z)} \frac{dF(z)}{dz} \right) - 2F(z) \frac{d^2r(z)}{dz^2} \right] \left(\frac{\partial^2}{\partial z \partial x} h_t^y(\vec{x}, z) - \frac{\partial^2}{\partial z \partial y} h_t^x(\vec{x}, z) \right) \right\} \\ & + \frac{\lambda_A}{2\kappa^2} \int d^4x \left\{ \bar{\Theta}_A(z) \frac{d\Phi(z)}{dz} \left(\frac{\partial}{\partial x} a_y(\vec{x}, z) - \frac{\partial}{\partial y} a_x(\vec{x}, z) \right) \right\}. \end{aligned}$$

The quantity in the first [...] is a total derivative, so this part can be integrated by parts, which gives

$$\begin{aligned} & \frac{\lambda}{4\kappa^2} \int d^3x \bar{\Theta}(z) \frac{dr(z)}{dz} \left(r(z) \frac{dF(z)}{dz} - 2F(z) \frac{dr(z)}{dz} \right) \left(\frac{\partial}{\partial x} h_t^y(\vec{x}, z) - \frac{\partial}{\partial y} h_t^x(\vec{x}, z) \right) \Bigg|_{z=z_H}^{z=\infty} \\ & + \frac{\lambda}{4\kappa^2} \int d^4x \left\{ \bar{\Theta}(z) \left[- \frac{dr(z)}{dz} \left(r(z) \frac{dF(z)}{dz} - 2F(z) \frac{dr(z)}{dz} \right) + r(z)^3 \frac{d}{dz} \left(\frac{1}{r(z)} \frac{dF(z)}{dz} \right) \right] \right\} \end{aligned}$$

$$\begin{aligned}
& - 2r(z)F(z) \frac{d^2 r(z)}{dz^2} \left[\left(\frac{\partial^2}{\partial z \partial x} h_t^y(\vec{x}, z) - \frac{\partial^2}{\partial z \partial y} h_t^x(\vec{x}, z) \right) \right] \\
& + \frac{\lambda_A}{2\kappa^2} \int d^4 x \left\{ \bar{\Theta}_A(z) \frac{d\Phi(z)}{dz} \left(\frac{\partial}{\partial x} a_y(\vec{x}, z) - \frac{\partial}{\partial y} a_x(\vec{x}, z) \right) \right\}.
\end{aligned}$$

Combine this with (3.12), we have:

$$\begin{aligned}
S^{(1)} &= \frac{\lambda}{4\kappa^2} \int_{z=z_H} d^3 x \bar{\Theta}(z) \frac{dr(z)}{dz} \left(2F(z) \frac{dr(z)}{dz} - r(z) \frac{dF(z)}{dz} \right) \left(\frac{\partial}{\partial x} h_t^y(\vec{x}, z) - \frac{\partial}{\partial y} h_t^x(\vec{x}, z) \right) \\
&+ \frac{\lambda}{8\kappa^2} \int_{z=\infty} d^3 x \left\{ \bar{\Theta}(z) r(z) \left(2F(z) \frac{dr(z)}{dz} - r(z) \frac{dF(z)}{dz} \right) \left(\frac{\partial^2}{\partial z \partial x} h_t^y(\vec{x}, z) - \frac{\partial^2}{\partial z \partial y} h_t^x(\vec{x}, z) \right) \right\} \\
&+ \frac{\lambda}{4\kappa^2} \int d^4 x \left\{ \bar{\Theta}(z) \left[- \frac{dr(z)}{dz} \left(r(z) \frac{dF(z)}{dz} - 2F(z) \frac{dr(z)}{dz} \right) + r(z)^3 \frac{d}{dz} \left(\frac{1}{r(z)} \frac{dF(z)}{dz} \right) \right. \right. \\
&\quad \left. \left. - 2r(z)F(z) \frac{d^2 r(z)}{dz^2} \right] \left(\frac{\partial^2}{\partial z \partial x} h_t^y(\vec{x}, z) - \frac{\partial^2}{\partial z \partial y} h_t^x(\vec{x}, z) \right) \right\} \tag{3.13} \\
&+ \frac{\lambda_A}{2\kappa^2} \int d^4 x \left\{ \bar{\Theta}_A(z) \frac{d\Phi(z)}{dz} \left(\frac{\partial}{\partial x} a_y(\vec{x}, z) - \frac{\partial}{\partial y} a_x(\vec{x}, z) \right) \right\}.
\end{aligned}$$

This is the linearized action we will use in the next subsection to compute angular momentum.

3.3 Vector Mode Fluctuations and Angular Momentum Density

Since $S^{(1)}$ is already linear in spatial derivatives, we only need to solve equations for $h_t^i(\vec{x}, z)$ ($i = x, y$) at the homogeneous leading order. That is, we can view spatial derivatives as small quantities and solve only up to leading order in derivative expansion. There are four relevant equations for vector mode fluctuations: the tz -component of the linearized Einstein equation and the z -component of the linearized Maxwell equation

$$\frac{F(z)}{2r(z)^2} \frac{\partial}{\partial z} \left(\frac{r(z)^2}{F(z)} \partial_i h_t^i(\vec{x}, z) \right) = O(\bar{\partial}^2), \tag{3.14}$$

$$\frac{d\Phi(z)}{dz} \partial_i h_t^i(\vec{x}, z) + \frac{F(z)}{r(z)^2} \frac{\partial}{\partial z} (\partial_i a_i(\vec{x}, z)) = 0, \tag{3.15}$$

where sum over $i = x, y$ is understood, and the ti -component of the linearized Einstein equation and i -component of the linearized Maxwell equation

$$\frac{d}{dz} \left[r(z)^4 \left(\frac{d}{dz} h_t^i(\vec{x}, z) \right) + r(z)^2 \frac{d\Phi(z)}{dz} a_i(\vec{x}, z) \right] = O(\bar{\partial}), \tag{3.16}$$

$$r(z)^2 \frac{d\Phi(z)}{dz} \left(\frac{d}{dz} h_t^i(\vec{x}, z) \right) + \frac{d}{dz} \left[F(z) \frac{d}{dz} a_i(\vec{x}, z) \right] = O(\bar{\partial}). \tag{3.17}$$

Equation (3.14) can be directly integrated out, which gives

$$\frac{r(z)^2}{F(z)} \partial_i h_t^i(\vec{x}, z) = C_1(\vec{x}) + O(\bar{\partial}^2),$$

where $C_1(\vec{x})$ is an arbitrary function independent of z . Since the right hand side is already independent of z , the left hand side must also be independent of z . To achieve this, the z -dependence of $h_t^i(\vec{x}, z)$ must cancel the prefactor $r(z)^2/F(z)$. Noticing that this factor goes to 1 at the boundary, and we want to normalize $h_t^i(\vec{x}, z)$ at the boundary as $h_t^i(\vec{x}, z \rightarrow \infty) = \bar{h}_{ti}(\vec{x})$, we get the solution

$$h_t^i(\vec{x}, z) = \frac{F(z)}{r(z)^2} \bar{h}_{ti}(\vec{x}) + O(\vec{\partial}) . \quad (3.18)$$

Here indices of boundary fields \bar{h}_{ti} are raised and lowered by the 3-d flat Lorentzian metric $\eta_{\alpha\beta} = (-1, 1, 1)$. $C_1(\vec{x})$ is then determined accordingly. Plug this solution into equation (3.15) and integrate in out, we get

$$\partial_i \left(a_i(\vec{x}, z) + \Phi(z) \bar{h}_{ti}(\vec{x}) \right) = C_2(\vec{x}) + O(\vec{\partial}^2) ,$$

where $C_2(\vec{x})$ is an arbitrary function independent of z . Same as before, we want the left hand side to be z -independent. Noticing that $\Phi(z \rightarrow \infty) = \Phi_0 + O(z^{-1})$ and we want to normalize $a_i(\vec{x}, z)$ at the boundary as $a_i(\vec{x}, z \rightarrow \infty) = 0$, we get the solution

$$a_i(\vec{x}, z) = (\Phi_0 - \Phi(z)) \bar{h}_{ti}(\vec{x}) + O(\vec{\partial}) . \quad (3.19)$$

Using background EOMs it is straightforward to check that the solutions (3.18) and (3.19) solve the second order equations (3.16) and (3.17) as well. Thus the vector mode fluctuations are completely solved at the leading order in derivative expansion.

Plug these solutions into (3.13), and integrate by parts the bulk integrals, we arrive at

$$\begin{aligned} S^{(1)} &= -\frac{\lambda_A}{4\kappa^2} \int_{z=\infty} d^3x \bar{\Theta}_A(z) (\Phi_0 - \Phi(z))^2 \left(\frac{\partial}{\partial x} \bar{h}_{ty}(\vec{x}) - \frac{\partial}{\partial y} \bar{h}_{tx}(\vec{x}) \right) \\ &+ \frac{\lambda}{8\kappa^2} \int_{z=z_H} d^3x \bar{\Theta}(z) \frac{dF(z)}{dz} \left(2 \frac{F(z)}{r(z)} \frac{dr(z)}{dz} - \frac{dF(z)}{dz} \right) \left(\frac{\partial}{\partial x} \bar{h}_{ty}(\vec{x}) - \frac{\partial}{\partial y} \bar{h}_{tx}(\vec{x}) \right) \\ &+ \frac{\lambda_A}{4\kappa^2} \int_{z=z_H} d^3x \bar{\Theta}_A(z) (\Phi_0 - \Phi(z))^2 \left(\frac{\partial}{\partial x} \bar{h}_{ty}(\vec{x}) - \frac{\partial}{\partial y} \bar{h}_{tx}(\vec{x}) \right) \\ &- \frac{\lambda}{8\kappa^2} \int d^4x r(z)^4 \left[\frac{d}{dz} \left(\frac{F(z)}{r(z)^2} \right) \right]^2 \frac{d\bar{\Theta}(z)}{dz} \left(\frac{\partial}{\partial x} \bar{h}_{ty}(\vec{x}) - \frac{\partial}{\partial y} \bar{h}_{tx}(\vec{x}) \right) \\ &+ \frac{\lambda_A}{4\kappa^2} \int d^4x (\Phi_0 - \Phi(z))^2 \frac{d\bar{\Theta}_A(z)}{dz} \left(\frac{\partial}{\partial x} \bar{h}_{ty}(\vec{x}) - \frac{\partial}{\partial y} \bar{h}_{tx}(\vec{x}) \right) . \end{aligned}$$

Noticing $F(z) = 4\pi T(z - z_H) + O((z - z_H)^2)$ and $\Phi(z) = O(z - z_H)$ near the horizon and $\Phi(z \rightarrow \infty) = \Phi_0 + O(z^{-1})$ near the boundary, we get

$$\begin{aligned} S^{(1)} &= \frac{1}{2\kappa^2} \left(\frac{1}{2} \Phi_0^2 \lambda_A \bar{\Theta}_A(z_H) - 4\pi^2 T^2 \lambda \bar{\Theta}(z_H) \right) \int d^3x \left(\frac{\partial}{\partial x} \bar{h}_{ty}(\vec{x}) - \frac{\partial}{\partial y} \bar{h}_{tx}(\vec{x}) \right) \\ &+ \frac{1}{2\kappa^2} \int_{z_H}^{\infty} dz \left[\frac{\lambda_A}{2} (\Phi_0 - \Phi(z))^2 \frac{d\bar{\Theta}_A(z)}{dz} \right] \int d^3x \left(\frac{\partial}{\partial x} \bar{h}_{ty}(\vec{x}) - \frac{\partial}{\partial y} \bar{h}_{tx}(\vec{x}) \right) \end{aligned}$$

$$+ \frac{1}{2\kappa^2} \int_{z_H}^{\infty} dz \left\{ -\frac{\lambda}{4} r(z)^4 \left[\frac{d}{dz} \left(\frac{F(z)}{r(z)^2} \right) \right]^2 \frac{d\bar{\Theta}(z)}{dz} \right\} \int d^3x \left(\frac{\partial}{\partial x} \bar{h}_{ty}(\vec{x}) - \frac{\partial}{\partial y} \bar{h}_{tx}(\vec{x}) \right).$$

Compare with the formula (3.7), we get

$$\begin{aligned} \ell = & \frac{\lambda_A}{2\kappa^2} \left\{ \Phi_0^2 \Theta_A [\theta(z_H)] + \int_{z_H}^{\infty} dz (\Phi_0 - \Phi(z))^2 \frac{d\Theta_A [\theta(z)]}{dz} \right\} \\ & - \frac{\lambda}{4\kappa^2} \left\{ 16\pi^2 T^2 \Theta [\theta(z_H)] + \int_{z_H}^{\infty} dz r(z)^4 \left[\frac{d}{dz} \left(\frac{F(z)}{r(z)^2} \right) \right]^2 \frac{d\Theta [\theta(z)]}{dz} \right\}, \quad (3.20) \end{aligned}$$

where $\Phi_0 = \Phi(z = \infty)$.

This result is in agreement with that obtained in [33].⁴ The basic concept behind the method here and that in [33] are the same, which is to look at the momentum density 1-point function's response to spatially inhomogeneous perturbations. But the executions of the computation are done in different ways. In [33] the inhomogeneous momentum density are obtained by directly solving inhomogeneous bulk equations of motion. While here by looking at first order action's response rather than that of momentum density itself and performing an integration by parts, we obtain the template formula (3.7). The spatial derivative is shifted from the momentum density to the metric fluctuation. Then to calculate the homogeneous angular momentum density, technically we only need to solve homogeneous bulk equations which is very easy to do. The results of course agree as we have checked explicitly here, because the integration by parts in the action is just a mathematical trick and should not have any physical consequence.

3.4 Effective Masses and Membrane Paradigm Violation

From (3.20), we can see that in general both gauge and gravitational Chern-Simons terms contribute to the angular momentum density. The contributions are not just from the horizon area, as opposed to many transport coefficients such as the shear and Hall viscosities, which we will compute in the next section. The fact that parts of the contribution are written as integrals from the horizon to the boundary suggests that the IR degrees of freedom interact non-trivially with the UV degrees of freedom to generate the angular momentum density.

⁴To go from our expression to that of [33], one first need to substitute in the following field and coupling redefinition:

$$A_\mu \Rightarrow LA_\mu, \quad \lambda_A \Rightarrow -4\beta_{CS}, \quad \lambda \Rightarrow \alpha_{CS} L^2, \quad \Theta_A [\vartheta], \Theta [\vartheta] \Rightarrow \vartheta,$$

where on the right hand side of “ \Rightarrow ” are the notations of [33] (the AdS radius L is denoted by ℓ there, but to avoid confusion, we will still use L here). This implies $\Phi_0 \Rightarrow L\mu$. After these substitution, our actions take exactly the same form as those used in [33]. Next, to transform the metric to that of [33], we redefine the coordinate system as

$$r(z) = \frac{L}{\xi}, \quad F(z) = f(\xi) \frac{L^2}{\xi^2}, \quad z = -L^2 \int \frac{\sqrt{f(\xi)h(\xi)}}{\xi^2} d\xi.$$

Now one can check our metric (2.22) takes the form of eq. (1.4) in [33], where their AdS radius coordinate “ z ” is re-denoted by ξ here to avoid conflict of symbols. Next it is straightforward to substitute these expressions into (3.20) and see that it takes exactly the same form as eqs. (1.5) and (1.6) in [33]. Notice that the upper integral limit of ∞ here shall be replaced by 0 as $\xi = 0$ is the AdS boundary in [33].

In the so-called membrane paradigm [42], many zero-frequency and zero-momentum linear response transport coefficients can be expressed completely in terms of geometric quantities evaluated at the black hole horizon in holographic dual. But here the angular momentum density (3.20) is clearly an exception. One key ingredient in the derivation of the membrane paradigm in [42] is that the bulk degrees of freedom associated with the linear response in question is massless, thus the bulk equations of motion can be integrated out which yields the membrane paradigm. But when a mass term is included (or generated) in the equations of motion, it usually spoils the integrability thus can break the membrane paradigm. This is what happens here to the angular momentum density. Although the vector mode fluctuations we are considering here originate from massless bulk fluctuations, they acquire effective z -dependent masses spontaneously from the non-trivial profile of $\Phi(z)$ and the geometry. We will show in the following that equations (3.16) and (3.17) are actually equations of motion for massive vector fluctuations.

First, we notice that the background equation (2.25) can be solved formally:

$$\Phi(z) = \Phi_0 - \frac{\Phi_1}{L^2} \int_{\infty}^z \frac{d\xi}{r(\xi)^2}, \quad \text{with} \quad \Phi_1 = -\Phi_0 L^2 \left(\int_{z_H}^{\infty} \frac{d\xi}{r(\xi)^2} \right)^{-1}. \quad (3.21)$$

In fact, up to normalization factors, $\Phi_0 = \mu$ and $\Phi_1 = -\rho$ where μ and ρ are the chemical potential and charge density of the system. Now using the properties of the solutions (3.18) and (3.19)

$$\begin{aligned} a_i(\vec{x}, z) &= \frac{r(z)^2}{F(z)} [\Phi_0 - \Phi(z)] h_t^i(\vec{x}, z) + O(\vec{\partial}), \\ \frac{\partial}{\partial z} h_t^i(\vec{x}, z) &= h_t^i(\vec{x}, z) \frac{\partial}{\partial z} \log \frac{F(z)}{r(z)^2} + O(\vec{\partial}), \end{aligned}$$

we can manipulate the second term in (3.16) to get the following form

$$\frac{d}{dz} \left[r(z)^4 \left(\frac{d}{dz} h_t^i(\vec{x}, z) \right) \right] - \frac{\Phi_1^2 L^{-4}}{F(z)} h_t^i(\vec{x}, z) = O(\vec{\partial}). \quad (3.22)$$

In this equation, the first term is the equation of motion for massless vector mode fluctuation of the metric as usual, but the second term corresponds to an effective mass term⁵ with a z -dependent mass square:

$$m_h^2(z) = \frac{\Phi_1^2 L^{-4}}{r(z)^4}. \quad (3.23)$$

Similarly manipulating the first term in (3.17) it becomes

$$\frac{d}{dz} \left[F(z) \frac{d}{dz} a_i(\vec{x}, z) \right] - \left[\frac{d}{dz} \left(\frac{F(z)}{r(z)^2} \right) \right] \left(\int_{\infty}^z \frac{d\xi}{r(\xi)^2} \right)^{-1} a_i(\vec{x}, z) = O(\vec{\partial}). \quad (3.24)$$

The first term in the above equation corresponds to that of massless Maxwell field and the second term an effective Proca mass term with a z -dependent mass square:

$$m_a^2(z) = \left[\frac{d}{dz} \left(\frac{F(z)}{r(z)^2} \right) \right] \left(\int_{\infty}^z \frac{d\xi}{r(\xi)^2} \right)^{-1}. \quad (3.25)$$

⁵To read off the value of mass, this can be compared, for example, with eqs. (2.49) and (2.50) in [43].

Then (3.20) can be written as

$$\begin{aligned} \ell = & \frac{\lambda_A}{2\kappa^2} \left\{ \Phi_0^2 \Theta_A [\theta(z_H)] + \int_{z_H}^{\infty} dz m_h^2(z) r(z)^4 \left(\int_{\infty}^z \frac{d\xi}{r(\xi)^2} \right)^2 \frac{d\Theta_A [\theta(z)]}{dz} \right\} \\ & - \frac{\lambda}{4\kappa^2} \left\{ 16\pi^2 T^2 \Theta [\theta(z_H)] + \int_{z_H}^{\infty} dz [m_a^2(z)]^2 r(z)^4 \left(\int_{\infty}^z \frac{d\xi}{r(\xi)^2} \right)^2 \frac{d\Theta [\theta(z)]}{dz} \right\}. \end{aligned} \quad (3.26)$$

Now we can see that the two integral terms which violate the membrane paradigm form have the same structure: the integrands are product of effective masses of the vector fluctuations and non-trivial radial flows of the axion profile. These two factors are the two sources of the membrane paradigm violation. Near the boundary

$$m_h^2(z \rightarrow \infty) \rightarrow \frac{\Phi_1^2}{z^4}, \quad m_a^2(z \rightarrow \infty) \rightarrow \frac{3\Gamma}{z^3},$$

the fluctuations become massless, as expected.

4 Tensor Mode Fluctuations and Hall Viscosity

The Hall viscosity for gravitational Chern-Simons model with an axion coupling has been computed in [27, 28], but in a different form of the metric. Here, for completeness, we present the derivation again, appropriate for the background ansatz (2.22). The result we will derive here is also a generalization of the results in [27, 28], since we have a generic Chern-Simons coupling function $\Theta[\vartheta]$ in (2.7). In this section, for computing viscosities, we only consider the homogeneous case where all the fluctuations are independent of spatial coordinates x and y . In this case, the tensor mode fluctuations h_{xy} and $h_{xx} - h_{yy}$ decouple from the rest.

4.1 Tensor Mode EOMs and Solutions

First we define:

$$h_{xy}(t, z) = r(z)^2 h_e(t, z), \quad \frac{1}{2} (h_{xx}(t, z) - h_{yy}(t, z)) = r(z)^2 h_o(t, z), \quad (4.1)$$

where the subscripts e and o mean even and odd under parity operation $x \leftrightarrow y$. We define the notations ϵ_{ij} ($i = e, o$) as following: $\epsilon_{eo} = -\epsilon_{oe} = 1$, $\epsilon_{ee} = \epsilon_{oo} = 0$. The the linearized Einstein equations for these fluctuations (in momentum space) are

$$\frac{d}{dz} \left[r(z)^2 F(z) \left(\frac{d}{dz} h_i(\omega, z) \right) \right] + \omega^2 \frac{r(z)^2}{F(z)} h_i(\omega, z) = \Xi_i(\omega, z; \lambda), \quad (4.2)$$

where

$$\Xi_i(\omega, z; \lambda) = -\frac{i}{2} \omega \lambda \epsilon_{ij} \left\{ -2 \frac{d}{dz} \left[r(z)^2 F(z) \frac{d\bar{\Theta}(z)}{dz} \left(\frac{d}{dz} h_j(\omega, z) \right) \right] \right\} \quad (4.3)$$

$$\left\{ \left[r(z)^2 \frac{d}{dz} \left(\frac{dF(z)}{dz} \frac{d\bar{\Theta}(z)}{dz} \right) - 2F(z) \frac{d}{dz} \left(r(z) \frac{dr(z)}{dz} \frac{d\bar{\Theta}(z)}{dz} \right) \right] h_j(\omega, z) \right\} \\ + i\omega^3 \lambda \frac{r(z)^2}{F(z)} \frac{d\bar{\Theta}(z)}{dz} \epsilon_{ij} h_j(\omega, z)$$

and the repeated index j is summed over e and o . The incoming wave solution is

$$h_i(\omega, z) = \left(\frac{z - z_H}{z} \right)^{-i \frac{\omega}{4\pi T}} \left[\bar{h}_i + i\omega h_i^{(1)}(z) + O(\omega^2) \right], \quad (4.4)$$

where

$$h_i^{(1)}(z) = \bar{h}_i \left[\frac{1}{4\pi T} \ln \left(\frac{z - z_H}{z} \right) - r(z_H)^2 \int_{\infty}^z d\xi \frac{1}{r(\xi)^2 F(\xi)} \right] \\ + \lambda \epsilon_{ij} \bar{h}_j \left\{ 2\pi T r(z_H)^2 \bar{\Theta}'(z_H) \int_{\infty}^z d\xi \frac{1}{r(\xi)^2 F(\xi)} \right. \\ \left. - \frac{1}{2} \int_{\infty}^z d\xi \left[\frac{d}{d\xi} \ln \left(\frac{F(\xi)}{r(\xi)^2} \right) \right] \frac{d\bar{\Theta}(\xi)}{d\xi} \right\}. \quad (4.5)$$

Because $\theta(z)$ is sourceless near the boundary: $\theta(z) \sim z^{-\Delta+}$, for a general $\Theta[\vartheta] = \vartheta^n$ ($n \geq 1$) near the boundary, the last line in the above equation goes to zero faster than $O(z^{-3})$ near the boundary, so only the second line contributes to Hall viscosity.

4.2 2-Point Functions and Viscosities

The total second order on-shell action for the tensor mode, from (2.16) and the corresponding boundary terms, is

$$S^{(2)} = \frac{1}{4\kappa^2} \int_{z=\infty} d^3x \sum_{i,j=e,o} \left\{ \left[\frac{4}{L} r(z)^2 \sqrt{F(z)} - \frac{d}{dz} (r(z)^2 F(z)) \right] h_i^2 - r(z)^2 F(z) h_i \left(\frac{\partial}{\partial z} h_i \right) \right. \\ + \frac{\lambda}{2} \epsilon_{ij} \left[r(z)^4 \left(\frac{d}{dz} \frac{F(z)}{r(z)^2} \right) \frac{d\bar{\Theta}(z)}{dz} h_i \left(\frac{\partial}{\partial t} h_j \right) + 2 \frac{r(z)^2}{F(z)} \bar{\Theta}(z) \left(\frac{\partial^2}{\partial t^2} h_i \right) \left(\frac{\partial}{\partial t} h_j \right) \right. \\ \left. \left. + 2r(z) \frac{dr(z)}{dz} F(z) \bar{\Theta}(z) \left(\frac{\partial}{\partial t} h_i \right) \left(\frac{\partial}{\partial z} h_j \right) - 2r(z)^3 F(z) \left(\frac{d}{dz} \frac{\bar{\Theta}(z)}{r(z)} \right) h_i \left(\frac{\partial^2}{\partial t \partial z} h_j \right) \right] \right\}. \quad (4.6)$$

Following the holographic prescriptions of [44–46], we obtain the 2-point functions in momentum space:

$$G_{\text{ra}}^{xy,xy}(\omega) = -\frac{\Gamma}{2\kappa^2 L^2} - i\omega \frac{r(z_H)^2}{2\kappa^2} + O(\omega^2), \quad (4.7)$$

$$G_{\text{ra}}^{xx-yy,xy}(\omega) = -i\omega \frac{2\pi T \lambda}{\kappa^2} r(z_H)^2 \bar{\Theta}'(z_H) + O(\omega^2). \quad (4.8)$$

Comparing with Kubo formulae [38]:⁶

$$G_{\text{ra}}^{xy,xy}(\omega) = p - i\omega\eta + O(\omega^2), \quad (4.9)$$

$$G_{\text{ra}}^{xx-yy,xy}(\omega) = 2i\omega\eta_H + O(\omega^2), \quad (4.10)$$

we get the shear viscosity

$$\frac{\eta}{s} = \frac{1}{4\pi}, \quad (4.11)$$

where the entropy density is $s = \frac{2\pi}{\kappa^2}r(z_H)^2$, and the Hall viscosity

$$\eta_H = -\frac{\lambda}{4\kappa^2} \left\{ r(z)^4 \left[\frac{d}{dz} \left(\frac{F(z)}{r(z)^2} \right) \right] \frac{d\Theta[\theta(z)]}{dz} \right\} \Bigg|_{z=z_H} = -\frac{\pi T\lambda}{\kappa^2} r(z_H)^2 \bar{\Theta}'(z_H), \quad (4.12)$$

where $\bar{\Theta}'(z) \equiv \partial_z \Theta[\theta(z)]$. The middle part in the above equation is from the first term in the second line of (4.6) and we have used $F(z) = 4\pi T(z - z_H) + O((z - z_H)^2)$ to go to right hand side. The Hall viscosity has a simple form which is expressed purely in terms of bulk quantities at the horizon. This is a generalization of results in [27, 28], for a generic gravitational Chern-Simons term of form (2.7). The gauge Chern-Simons term (2.4) has no contribution. The reason is obvious: this term is totally independent of the metric; since Hall viscosity is a response to the metric perturbation, it is natural that the gauge Chern-Simons has no contribution. In contrary to the membrane paradigm of the Hall viscosity, the angular momentum density (3.20) has a more complicated form: part of it does have a membrane paradigm form while the rest is an non-trivial bulk integral. This difference indicates that the physics behind these two quantities are different (at least for the holographic Chern-Simons models studied in this paper and the dual field theories they describe), thus in general, we expect their ratio to have some non-trivial behavior. This is difficult to study analytically. In the next section, we will present the numeric results.

5 Numeric Results of the Axion Condensate Phase

In this section, we numerically study Hall viscosity, angular momentum density and their ratio in terms of physical parameters such as temperature T and charge density ρ (we will use Canonical ensemble in this section, where ρ is held fixed) in the axion condensate phase of the holographic Chern-Simons model. In this phase, as the temperature is lowered, the axion scalar ϑ develops a non-trivial profile in the bulk and thus breaks the parity spontaneously. The order parameter corresponds to the expectation value $\langle \mathcal{O} \rangle$ of the operator \mathcal{O} in the field theory that is dual to the scalar ϑ . We will first work in the probe limit, and then include full back-reactions.

From (3.20) we see that angular momentum density receive contributions from both gauge and gravitational Chern-Simons terms. However, from (4.12), Hall viscosity is only

⁶The η_H term differs by a sign from [38] because our convention is $\epsilon_{txy} = 1$ in 3-d flat Minkowskian space (the boundary), which follows from $\epsilon_{txyz} = \sqrt{-g}$ in 4-d bulk space.

determined by the gravitational Chern-Simons term. In general, the two Chern-Simons coupling functions $\lambda_A \Theta_A[\vartheta]$ and $\lambda \Theta[\vartheta]$ can be different and unrelated. To make our analysis simple, from now on in most of this section, we will focus only on the gravitational Chern-Simons term, and turn off the gauge Chern-Simons term $\lambda_A = 0$. Only at the end of this section will we include the numeric result for the angular momentum density from the gauge Chern-Simons model.

Before starting the numeric analysis, we would like to first discuss the choice of the general function $\Theta[\vartheta]$ in (2.7). There is no unique choice for its form from the phenomenological model we write down here. When $\Theta[\vartheta] = \text{constant}$, the gravitational Chern-Simons term (2.7) is a boundary term because the Pontryagin density is a total derivative. This is not the case we are interested here, because we want this term to be dynamical, at least to have a non-trivial z -profile to generate non-vanishing Hall viscosity. In [27–29], the authors chose $\Theta[\vartheta] = \vartheta$, which results in the near-critical behavior of Hall viscosity to be $\eta_H \sim (T_c - T)^{1/2}$, because the Hall viscosity is linear to the condensate $\theta \sim \langle \mathcal{O} \rangle \sim (T_c - T)^{1/2}$. Another form, $\Theta[\vartheta] = \vartheta^2$, is also interesting, because from (3.20) and (4.12), both Hall viscosity and angular momentum density are quadratic in order parameter $\langle \mathcal{O} \rangle$ now, so near critical regime they will scale as $T_c - T$, instead of $(T_c - T)^{1/2}$. This is in agreement with condensed matter theory arguments such as in $p_x + ip_y$ paired states of BCS theory: since both Hall viscosity and angular momentum density have dimension $1/[\text{length}]^2$, by dimensional analysis, they are proportional to square of the order parameter, thus scale as $T_c - T$ near critical regime. Of course $\Theta[\vartheta]$ can take other forms in general. For $\Theta[\vartheta] = \vartheta^n$, Hall viscosity and angular momentum density will scale as $(T_c - T)^{n/2}$ near critical regime and η_H/ℓ will acquire a factor of n . When $\Theta[\vartheta]$ contains multiple terms of ϑ with different powers, the lowest power will dominate the near-critical behavior and the highest power the low temperature behavior. In this section we choose

$$\Theta[\vartheta] = \vartheta^2 \tag{5.1}$$

so as to reproduce the $T_c - T$ scaling near the critical regime.

5.1 Gravitational Chern-Simons Model: The Probe Limit

In this subsection we study the probe limit of the bulk theory, where the scalar field ϑ does not back-react on the metric and Maxwell field. This limit has been employed in [28, 29]. The background now is the AdS-Reissner-Nordström black hole:

$$\begin{cases} r(z) = \frac{z}{L} \\ F(z) = \left(\frac{z}{L}\right)^2 - \left(1 + \frac{Q^2}{4}\right) \frac{z_H^3}{L^2 z} + \frac{Q^2 z_H^4}{4L^2 z^2}, \\ \Phi(z) = Q \frac{z_H}{L} \left(1 - \frac{z_H}{z}\right) \end{cases} \tag{5.2}$$

where Q is the dimensionless charge. The temperature is

$$T = \frac{3z_H}{4\pi L^2} \left(1 - \frac{Q^2}{12}\right), \tag{5.3}$$

and to make the temperature non-negative, the charge has to satisfy $Q^2 \leq 12$. The near-boundary behavior of the scalar field is

$$\theta(z) \rightarrow \frac{\langle \mathcal{O} \rangle}{z^{\Delta_+}}, \quad (5.4)$$

and that of the electric potential is

$$\Phi(z) = \mu - \frac{\rho}{z} + O\left(\frac{1}{z^2}\right), \quad (5.5)$$

where $\langle \mathcal{O} \rangle$ is the condensate, μ the chemical potential and ρ the charge density (up to some factors of κ and L). Mass m is related to the conformal dimension Δ_+ of the condensate operator \mathcal{O} by (3.11). It has been shown in [28] that in this setup the black hole can develop a scalar hair only at very low temperature, where it is near extremal and the extremality factor $1 - Q^2/12$ is close to zero. Figure (1) shows numeric results for $c_4 L^2 = 0.5$ with various values of m . It is interesting to notice that despite the seemingly different analytic expressions for Hall viscosity and angular momentum density, their ratio η_H/ℓ remains more or less unchanged for a vast range of temperature until one reaches the very low temperature regime. However, the value of the ratio is typically a huge number depending on the mass m (or conformal dimension Δ_+) of the scalar condensate, and is far away from the $1/2$ value found in condensed matter literature. We will see that this feature remains when full back-reactions are included.

The stability for a charged black hole with a neutral scalar condensation was discussed in [47] as well as in [28,29]. In this paper when talking about neutral scalar condensation, we always focus on a narrow window around $m^2 L^2 = -2$, which is within the range discussed in these references and the black hole can develop a neutral scalar hair which condenses near the horizon.

5.2 Gravitational Chern-Simons Model: Including Back-reactions

The probe limit usually works well in high temperature when the black hole is far from extremal, and the condensate is small and the back-reactions are weak. However, in the probe limit of the previous subsection, numerics shows that the scalar can only condense when the black hole is near-extremal. But in this case the back-reactions play a very important role, thus the probe limit assumption may not be consistent. Particularly, Hall viscosity is solely expressed in terms of quantities near the horizon and so is part of the angular momentum density, thus the accuracy of the numeric solutions near the horizon matters a lot. Even in high temperature, when the back-reactions are negligible near the boundary and not strong in most part of the bulk, they are still very important near the horizon. For example, $r(z)$ has significant deviation from its probe limit form near the horizon. To improve the accuracy of the numeric results, in this subsection we will take back-reactions into full account.

Figure (2) shows the numeric results when full back-reactions are included. The mass is chosen to be $m^2 L^2 = -2$, corresponding to conformal dimension $\Delta_+ = 2$. The black dashed line is the linear case with $c_4 = 0$. The colored lines show non-linear effect, with bigger non-linear coefficient c_4 toward the red end. The non-linearity decreases the values of the condensate, Hall viscosity and angular momentum density. Numerically we find that below

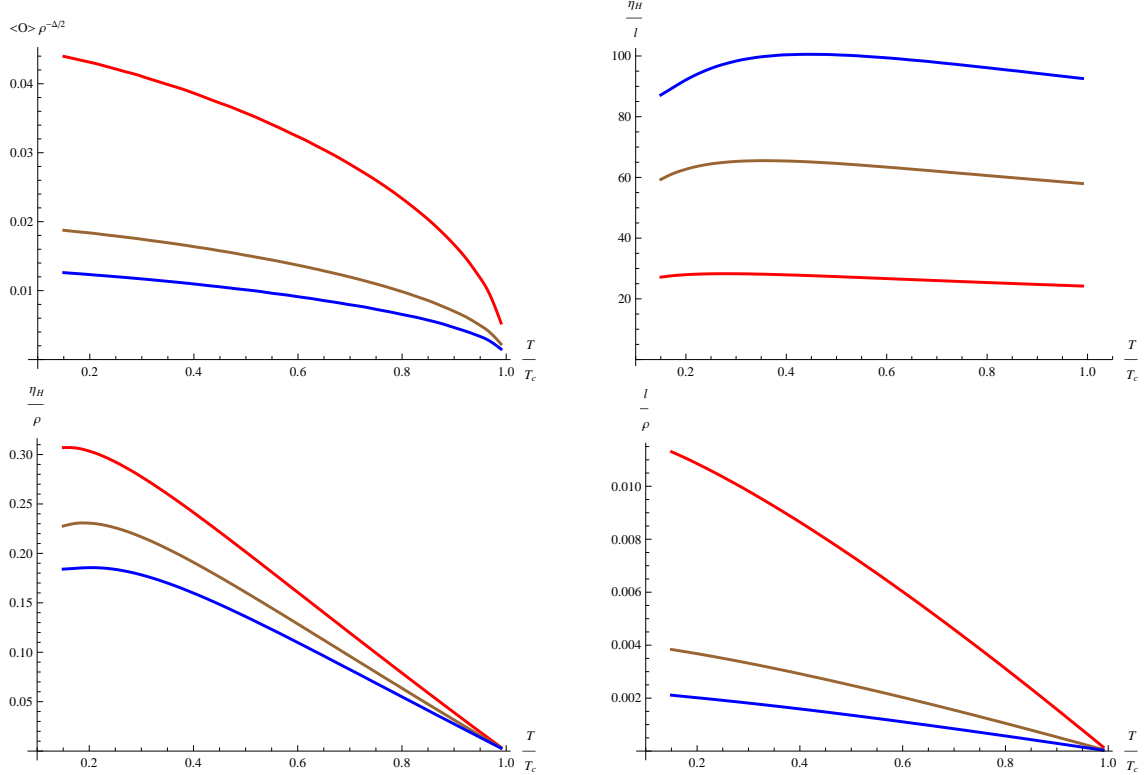


Figure 1: Condensate $\langle \mathcal{O} \rangle$ (upper left), Hall viscosity η_H (lower left), angular momentum density ℓ (lower right) and their ratio η_H/ℓ (upper right) as functions of T/T_c in the probe limit, with $c_4 L^2 = 0.5$. The red, brown and blue lines correspond to $m^2 L^2 = -2.2, -2.1$ and -2.05 , respectively. We have set $L = \lambda = \kappa = 1, \lambda_A = 0$.

certain low temperature ($< 0.3T_c$) it is hard to find a condensate solution when $c_4 > 0$: that is the reason why all the colored curves terminate at some low temperature.

The ratio between Hall viscosity and angular momentum density η_H/ℓ remains more or less unchanged at high temperature, same as in the probe limit. It only starts to drop off dramatically once gets to low temperature regime where $T < 0.3T_c$. It is not clear to us whether there is a physical origin or interpretation of the wiggles in the plot. Non-linearity has almost no effect near the critical temperature, because here the condensate is close to zero and the non-linear term is of higher order. It will only show up when the temperature is lowered and the condensate becomes large enough such that the non-linear term is comparable to the other terms. The non-linearity does decrease the ratio, however, its effect to the ratio is much weaker compared to that to Hall viscosity and angular momentum density individually. The numeric plot suggests that the non-linear effect on the η_H/ℓ ratio is at its strongest at the mid-temperature regime where $T \approx 0.5T_c$. As the temperature is lowered further, the non-linear effect on the ratio shows a trend to become weaker as the colorful lines get closer. It is interesting to notice that as the temperature drops below $T \approx 0.2T_c$, the ratio decrease dramatically towards zero. Due to the difficulties of numeric calculation for extremely low temperature regime, we can only work out the dashed line ($c_4 = 0$) below $T \approx 0.25T_c$ and can not go beyond $T \lesssim 0.1T_c$. It will be interesting to see whether at zero temperature the

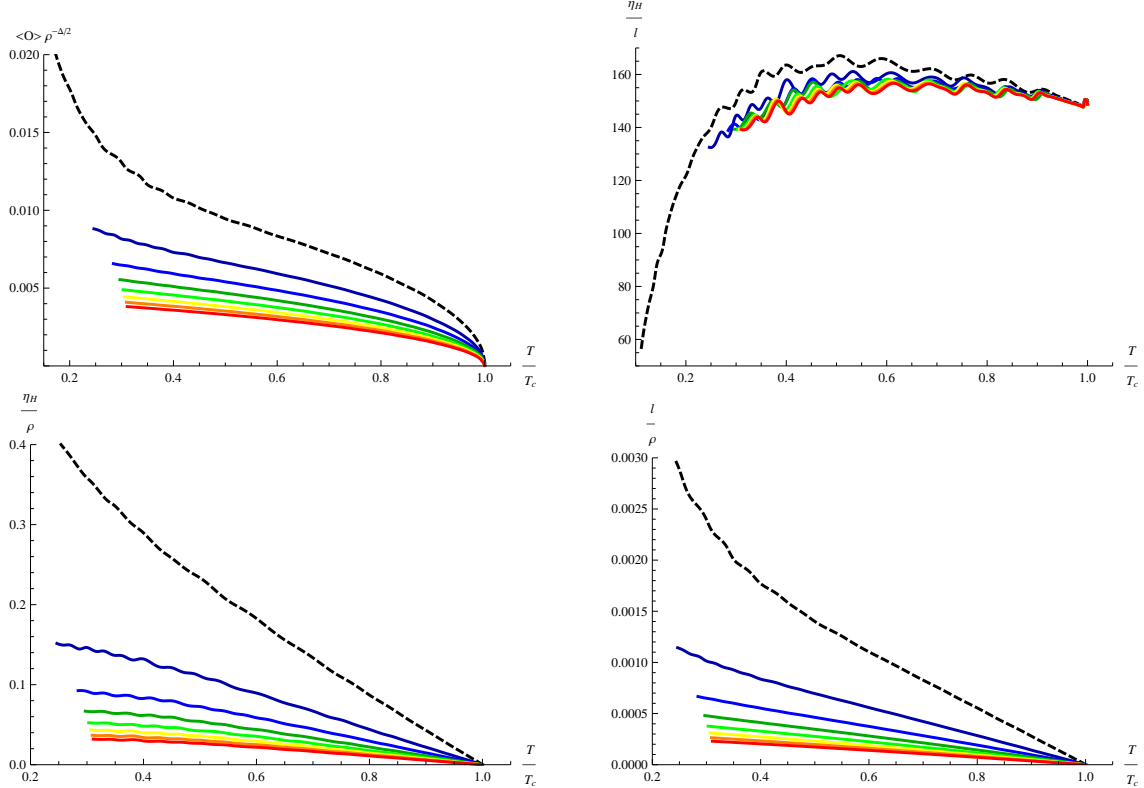


Figure 2: Condensate $\langle \mathcal{O} \rangle$ (upper left), Hall viscosity η_H (lower left), angular momentum density ℓ (lower right) and their ratio η_H/ℓ (upper right) as functions of T/T_c , with full back-reactions included. Here $m^2 L^2 = -2$, corresponding to conformal dimension $\Delta_+ = 2$. The black dashed line has $c_4 L^2 = 0$, with an increment of 0.25 for each adjacent line toward the red one, which has $c_4 L^2 = 1.75$. We have set $L = \lambda = \kappa = 1$, $\lambda_A = 0$.

ratio approaches some non-zero fixed value, for example, $1/2$ widely found in the study of field theory and condensed matter systems [7, 9, 13, 14, 16]. In this regime, the near horizon geometry may have different scalings than the $\text{AdS}_2 \times \mathbb{R}^2$ of extremal black holes, such as a AdS_2 with a different radius, and across a critical conformal dimension $m_c^2 L^2 = -3/2$ when T_c reaches zero, the system may undergo a Berezinskii-Kosterlitz-Thouless type phase transition with an exponentially generated scaling [47]. We will leave the study on zero temperature regime to the future.

The ratio also depends on the mass m (the conformal dimension Δ_+) as in the probe limit. Since the non-linearity does not play an important role, to separate this effect, we can just study the ratio's dependence on the mass at the critical temperature. Figure (3) shows the near-critical η_H/ℓ ratio as a function of conformal dimension, with a fitting of the following form:

$$\left. \frac{\eta_H}{\ell} \right|_{T \rightarrow T_c} = e^{-26.8 \sqrt{\Delta_+(3-\Delta_+)+42.9}}, \quad (5.6)$$

i.e. this near-critical ratio depends on mass m exponentially.

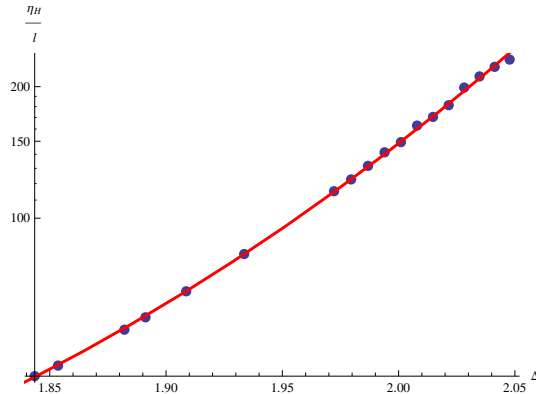


Figure 3: Hall viscosity to angular momentum density ratio η_H/ℓ near the critical regime $T \rightarrow T_c$ as a function of conformal dimension Δ_+ . $c_4 L^2 = \frac{1}{120}$. The dots are the numeric data and the red line is the fitting of (5.6). The vertical axis is shown in logarithmic scale.

5.3 Gauge Chern-Simons Model: Angular Momentum Density

At the end of this section, in Figure (4), we present the numeric result for the angular momentum density due to the gauge Chern-Simons term, i.e. the first line in (3.20). We turn off the gravitational Chern-Simons coupling: $\lambda = 0$ and choose $\Theta_A[\vartheta] = \vartheta^2$ as well. Qualitatively the plot is very similar to that of the gravitational Chern-Simons model.

Note added: After the original version of this paper, [34] appeared, where the angular momentum density, Hall viscosity and their ratio are studied analytically or numerically in a few classes of holographic models. The general form of the action they start with is the same as ours, with choices of different forms of the scalar potential $V[\vartheta]$. In the first class of models studied there, the non-normalizable mode of the scalar ϑ is turned on. This corresponds to turn on the source θ_0 here. In principle, the sourceless case we study in this section can be viewed as a limiting case as $\theta_0 \rightarrow 0$, given all other settings are the same in the $\theta_0 \neq 0$ case. Unfortunately this does not happen when we try to compare our results with those of [34], because other settings are not quite the same between ours and theirs. In our sourceless case, if the charge density μ and chemical potential ρ are turned off, the condensate $\theta(z) \neq 0$ can not form and both η_H and ℓ vanishes identically. In this case their ratio is simply not well defined (in other words, $0/0$ can be anything). Sections III.B and III.C of [34] consider cases without μ or ρ , but with source on. Although their η_H/ℓ does have a good limit as $\theta_0 \rightarrow 0$, this is not comparable to ours, and we suspect that the order of two limits $\theta_0 \rightarrow 0$ and $\mu, \rho \rightarrow 0$ may not be exchangeable, since they correspond to approaching the non-analytic point of $0/0$ of η_H/ℓ from different directions in the parameter space. For this same reason, results in section III.D and E are not immediately comparable either. Superficially, the case closest to what we study is section III.D, but only part of the angular momentum density, the non-integral part (called $\mathcal{J}_{\text{horizon}}$ there), is presented; the non-trivial integral part is omitted, thus a direct comparison is not available. In section IV of [34] the sourceless case is studied directly, this is the same as what we have studied in this section, where $\theta_0 = 0$ is imposed from the very beginning. But they turn on a non-trivial dilaton coupling $e^{-\alpha\vartheta}$ for the Maxwell term in the action, where we set it to unity. In their numeric computation, α is no less than

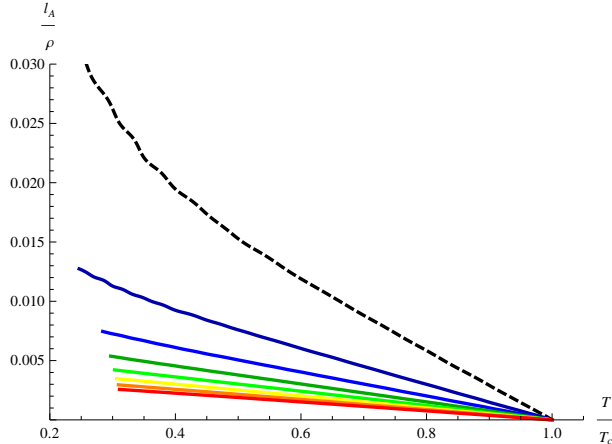


Figure 4: Angular momentum density ℓ as a function of T/T_c , with full back-reactions included. Here $m^2 L^2 = -2$, corresponding to conformal dimension $\Delta_+ = 2$. The black dashed line has $c_4 L^2 = 0$, with an increment of 0.25 for each adjacent line toward the red one, which has $c_4 L^2 = 1.75$. We have set $L = \lambda_A = \kappa = 1$, $\lambda = 0$.

0.5, thus a limiting case when $\alpha \rightarrow 0$ is not available for comparison. When α is finite, the dilaton coupling facilitates the formation of condensate: from their results we can see the non-trivial profile of ϑ can form at any temperature, especially at very high temperature; whereas for ours with $\alpha = 0$, it can only form below certain critical temperature T_c . Again this implies the high temperature (or small μ) limit and $\alpha \rightarrow 0$ limit may not be exchangeable when dilaton coupling is included. In summary, none of the cases studied in [34] encloses ours as a simple limiting case and they are complementary to what is studied in this section.

6 Conclusions and Comments

We have shown that holographic models with gauge and/or gravitational Chern-Simons terms have a non-vanishing angular momentum density when parity is broken by the scalar coupled to the Chern-Simons terms. Unlike Hall viscosity, the angular momentum density (3.20) does not have a membrane paradigm form: it is not solely determined by the near-horizon behavior of the background fields; part of it is an integral over the whole bulk regime outside the horizon, which suggests that the UV and IR degrees of freedom that are responsible for the generation of angular momentum density interact non-trivially with each other and do not decouple. These results are in agreement with those obtained in [33]. The effect of this angular momentum density is to accumulate momentum at the 1-dimensional spatial boundary of the 2+1-dimensional system, inducing an edge current of momentum whose strength is proportional to the angular momentum density, as shown in [38] and [33].

We have presented numeric results for the axion condensate phase of the gravitational Chern-Simons model when the scalar condensates, both at the probe limit and with back-reactions fully included. Both Hall viscosity and angular momentum density are monotonically decreasing functions of temperature. Non-linearity of the scalar potential $V[\vartheta]$ plays little role in asymptotic behaviors near the critical regime, but decreases both Hall viscosity

and angular momentum density below the critical temperature.

The Hall viscosity to angular momentum density ratio obtained numerically from the gravitational Chern-Simons term alone is not exactly a constant, but it does remain more or less unchanged for a vast range of temperature, except at the very low temperature regime. On the other hand, the ratio obtained from non-holographic approaches [7, 9, 13, 14, 16] is always 1/2. In fact, the apparently different forms of (4.12) and (3.20), and the facts that the former involves only gravitational Chern-Simons term and tensor mode metric fluctuations while the latter involves both gauge and gravitational Chern-Simons terms and only vector mode fluctuations, already suggest that the physical mechanisms of generating Hall viscosity and angular momentum density in holographic Chern-Simons models and the dual field theories they describe are quite different. Thus in general, a simple relationship between them would not be expected from these theories. How to understand the universal relation obtained from field theory and condensed matter theories and the non-universal results from holographic Chern-Simons models here (and what role the gauge Chern-Simons term plays regarding the relationship between Hall viscosity and angular momentum density) is still open questions to be answered in the future.

In this paper, we have obtained a general analytic formula (3.20) for angular momentum density. But numerically we have only studied the axion condensate phase where the AdS-Reissner-Nordström black hole develops a neutral scalar hair. At zero or very low temperature, the system may flow to different infrared geometries with different scalings [47, 48]. How the angular momentum density, Hall viscosity and their ratio behave in these different IR fixed points, is another interesting question that can be studied in the future.

Acknowledgments

The author is very grateful to Dam Thanh Son for inspiring discussions throughout the progress of this work, and thanks Nien-En Lee, Hong Liu, Hiroshi Ooguri, Nicholas Read, Bogdan Stoica and Paul Wiegmann for informative comments and useful email communications. The author thanks particularly the JHEP referee for very thoughtful comments and suggestions. This work is supported by DOE grant DE-FG02-90ER-40560 and NSF DMS-1206648.

References

- [1] K. Jensen, M. Kaminski, P. Kovtun, R. Meyer, A. Ritz and A. Yarom, “Parity-Violating Hydrodynamics in 2+1 Dimensions,” JHEP **1205**, 102 (2012) [[arXiv:1112.4498](#) [hep-th]].
- [2] M. Kaminski and S. Moroz, “Non-Relativistic Parity-Violating Hydrodynamics in Two Spatial Dimensions,” [arXiv:1310.8305](#) [cond-mat.mes-hall].
- [3] J. E. Avron, R. Seiler and P. G. Zograf, “Viscosity of quantum Hall fluids,” Phys. Rev. Lett. **75**, 697 (1995).

- [4] J. E. Avron, “Odd Viscosity,” *J. Stat. Phys.* **92**, 543 (1998) [[arXiv:physics/9712050](#)].
- [5] I. V. Tokatly and G. Vignale, “Lorentz shear modulus of a two-dimensional electron gas at high magnetic field,” *Phys. Rev. B* **76**, 161305 (2007) [[arXiv:0706.2454](#) [cond-mat.mes-hall]].
- [6] I. V. Tokatly and G. Vignale, “Lorentz shear modulus of fractional quantum Hall states,” [[arXiv:0812.4331](#) [cond-mat.mes-hall]].
- [7] N. Read, “Non-Abelian adiabatic statistics and Hall viscosity in quantum Hall states and paired superfluids,” *Phys. Rev. B* **79**, 045308 (2009) [[arXiv:0805.2507](#) [cond-mat.mes-hall]].
- [8] F. D. M. Haldane, “Hall viscosity’ and intrinsic metric of incompressible fractional Hall fluids,” [[arXiv:0906.1854](#) [cond-mat.str-el]].
- [9] N. Read and E. H. Rezayi, “Hall viscosity, orbital spin, and geometry: paired superfluids and quantum Hall systems,” *Phys. Rev. B* **84**, 085316 (2011) [[arXiv:1008.0210](#) [cond-mat.mes-hall]].
- [10] T. L. Hughes, R. G. Leigh and E. Fradkin, “Torsional Response and Dissipationless Viscosity in Topological Insulators,” *Phys. Rev. Lett.* **107**, 075502 (2011) [[arXiv:1101.3541](#) [cond-mat.mes-hall]].
- [11] T. L. Hughes, R. G. Leigh and O. Parrikar, “Torsional Anomalies, Hall Viscosity, and Bulk-boundary Correspondence in Topological States,” *Phys. Rev. D* **88**, 025040 (2013) [[arXiv:1211.6442](#) [hep-th]].
- [12] B. Bradlyn, M. Goldstein and N. Read, “Kubo formulas for viscosity: Hall viscosity, Ward identities, and the relation with conductivity,” *Phys. Rev. B* **86**, 245309 (2012) [[arXiv:](#) [cond-mat.stat-mech]].
- [13] C. Hoyos and D. T. Son, “Hall Viscosity and Electromagnetic Response,” *Phys. Rev. Lett.* **108**, 066805 (2012) [[arXiv:1109.2651](#) [cond-mat.mes-hall]].
- [14] A. Nicolis and D. T. Son, “Hall viscosity from effective field theory,” [[arXiv:1103.2137](#) [hep-th]].
- [15] C. Hoyos, S. Moroz and D. T. Son, “Effective theory of chiral two-dimensional superfluids,” [[arXiv:1305.3925](#) [cond-mat.quant-gas]].
- [16] D. T. Son, “Newton-Cartan Geometry and the Quantum Hall Effect,” [[arXiv:1306.0638](#) [cond-mat.mes-hall]].
- [17] Y. Hidaka, Y. Hirono, T. Kimura and Y. Minami, “Viscoelastic-electromagnetism and Hall viscosity,” *PTEP* **2013**, 013A02 (2013) [[arXiv:1206.0734](#) [cond-mat.mes-hall]].
- [18] P. B. Wiegmann, “Quantum Hydrodynamics of Fractional Hall Effect: Quantum Kirchhoff Equations,” [[arXiv:1211.5132](#) [cond-mat.str-el]].

- [19] P. B. Wiegmann, “Anomalous Hydrodynamics of Fractional Quantum Hall States,” JETP **144** (9), 617 (2013) [[arXiv:1305.6893](#) [cond-mat.str-el]].
- [20] P. B. Wiegmann, “Hydrodynamics of Euler incompressible fluid and the Fractional Quantum Hall Effect,” [arXiv:1309.5992](#) [cond-mat.str-el].
- [21] M. Stone and R. Roy, “Edge modes, edge currents, and gauge invariance in superfluids and superconductors,” Phys. Rev. B **69**, 184511 (2004) [[arXiv:cond-mat/0308034](#)].
- [22] J. A. Sauls, “Surface States, Edge Currents and the Angular Momentum of Chiral -wave Superfluids,” Phys. Rev. B **84**, 214509 (2011) [[arXiv:1209.5501](#) [cond-mat.supr-con]].
- [23] Y. Tsutsumi and K. Machida, “Edge mass current and the role of Majorana fermions in a-phase superfluid He-3,” Phys. Rev. B **85**, 100506 (2012).
- [24] J. M. Maldacena, “The Large N limit of superconformal field theories and supergravity,” Adv. Theor. Math. Phys. **2**, 231 (1998) [[hep-th/9711200](#)].
- [25] S. S. Gubser, I. R. Klebanov and A. M. Polyakov, “Gauge theory correlators from noncritical string theory,” Phys. Lett. B **428**, 105 (1998) [[hep-th/9802109](#)].
- [26] E. Witten, “Anti-de Sitter space and holography,” Adv. Theor. Math. Phys. **2**, 253 (1998) [[hep-th/9802150](#)].
- [27] O. Saremi and D. T. Son, “Hall viscosity from gauge/gravity duality,” JHEP **1204**, 091 (2012) [[arXiv:1103.4851](#) [hep-th]].
- [28] J. -W. Chen, N. -E. Lee, D. Maity and W. -Y. Wen, “A Holographic Model For Hall Viscosity,” Phys. Lett. B **713**, 47 (2012) [[arXiv:1110.0793](#) [hep-th]].
- [29] J. -W. Chen, S. -H. Dai, N. -E. Lee and D. Maity, “Novel Parity Violating Transport Coefficients in 2+1 Dimensions from Holography,” JHEP **1209**, 096 (2012) [[arXiv:1206.0850](#) [hep-th]].
- [30] R. -G. Cai, T. -J. Li, Y. -H. Qi and Y. -L. Zhang, “Incompressible Navier-Stokes Equations from Einstein Gravity with Chern-Simons Term,” Phys. Rev. D **86**, 086008 (2012)
- [31] D. -C. Zou and B. Wang, “Holographic parity violating charged fluid dual to Chern-Simons modified gravity,” [arXiv:1306.5486](#) [hep-th].
- [32] H. Liu, H. Ooguri, B. Stoica and N. Yunes, “Spontaneous Generation of Angular Momentum in Holographic Theories,” Phys. Rev. Lett. **110**, no. 21, 211601 (2013) [[arXiv:1212.3666](#) [hep-th]].
- [33] H. Liu, H. Ooguri and B. Stoica, “Angular Momentum Generation by Parity Violation,” Phys. Rev. D **89**, 106007 (2014) [[arXiv:1311.5879](#) [hep-th]].
- [34] H. Liu, H. Ooguri and B. Stoica, “Hall Viscosity and Angular Momentum in Gapless Holographic Models,” [arXiv:1403.6047](#) [hep-th].

- [35] F. Wilczek, “Two Applications of Axion Electrodynamics,” *Phys. Rev. Lett.* **58**, 1799 (1987).
- [36] S. M. Carroll, G. B. Field and R. Jackiw, “Limits on a Lorentz and Parity Violating Modification of Electrodynamics,” *Phys. Rev. D* **41**, 1231 (1990).
- [37] R. Jackiw and S. Y. Pi, “Chern-Simons modification of general relativity,” *Phys. Rev. D* **68**, 104012 (2003) [[gr-qc/0308071](#)].
- [38] D. T. Son and C. Wu, “Holographic Spontaneous Parity Breaking and Emergent Hall Viscosity and Angular Momentum,” *JHEP* **1407**, 076 (2014) [[arXiv:1311.4882](#) [hep-th]].
- [39] S. S. Gubser, “Colorful horizons with charge in anti-de Sitter space,” *Phys. Rev. Lett.* **101**, 191601 (2008) [[arXiv:0803.3483](#) [hep-th]].
- [40] M. M. Roberts and S. A. Hartnoll, “Pseudogap and time reversal breaking in a holographic superconductor,” *JHEP* **0808**, 035 (2008)
- [41] S. Alexander and N. Yunes, “Chern-Simons Modified General Relativity,” *Phys. Rept.* **480**, 1 (2009) [[arXiv:0907.2562](#) [hep-th]].
- [42] N. Iqbal and H. Liu, “Universality of the hydrodynamic limit in AdS/CFT and the membrane paradigm,” *Phys. Rev. D* **79**, 025023 (2009) [[arXiv:0809.3808](#) [hep-th]].
- [43] C. de Rham, “Massive Gravity,” *Living Rev. Rel.* **17**, 7 (2014) [[arXiv:1401.4173](#) [hep-th]].
- [44] C. P. Herzog and D. T. Son, “Schwinger-Keldysh propagators from AdS/CFT correspondence,” *JHEP* **0303**, 046 (2003) [[hep-th/0212072](#)].
- [45] E. Barnes, D. Vaman, C. Wu and P. Arnold, “Real-time finite-temperature correlators from AdS/CFT,” *Phys. Rev. D* **82**, 025019 (2010) [[arXiv:1004.1179](#) [hep-th]].
- [46] P. Arnold, D. Vaman, C. Wu and W. Xiao, “Second order hydrodynamic coefficients from 3-point stress tensor correlators via AdS/CFT,” *JHEP* **1110**, 033 (2011) [[arXiv:1105.4645](#) [hep-th]].
- [47] N. Iqbal, H. Liu, M. Mezei and Q. Si, “Quantum phase transitions in holographic models of magnetism and superconductors,” *Phys. Rev. D* **82**, 045002 (2010) [[arXiv:1003.0010](#) [hep-th]].
- [48] B. Gouteraux and E. Kiritsis, “Quantum critical lines in holographic phases with (un)broken symmetry,” *JHEP* **1304**, 053 (2013) [[arXiv:1212.2625](#) [hep-th]].